Vietnam Journal of Mechanics, VAST, Vol. 43, No. 2 (2021), pp. 139 – 170
DOI: https://doi.org/10.15625/0866-7136/15671

STOCHASTIC ANALYSIS OF LATTICE, NONLOCAL CONTINUOUS BEAMS IN VIBRATION

Yuchen Li[1], **Noël Challamel**[1,*], **Isaac Elishakoff**[2]
[1]*Université Bretagne Sud, UMR CNRS 6027, IRDL, F-56100 Lorient, France*
[2]*Department of Ocean and Mechanical Engineering, Florida Atlantic University, 777 Glades Road – EG 36/Rm 106, Boca Raton, FL 33431, United States*
[*]E-mail: noel.challamel@univ-ubs.fr

Received: 09 November 2020 / Published online: 28 June 2021

Abstract. In this paper, we study the stochastic behavior of some lattice beams, called Hencky bar-chain model and their non-local continuous beam approximations. Hencky bar-chain model is a beam lattice composed of rigid segments, connected by some homogeneous rotational elastic links. In the present stochastic analysis, the stiffness of these elastic links is treated as a continuous random variable, with given probability density function. The fundamental eigenfrequency of the linear difference eigenvalue problem is also a random variable in this context. The reliability is defined as the probability that this fundamental frequency is less than an excitation frequency. This reliability function is exactly calculated for the lattice beam in conjunction with various boundary conditions. An exponential distribution is considered for the random stiffness of the elastic links. The stochastic lattice model is then compared to a stochastic nonlocal beam model, based on the continualization of the difference equation of the lattice model. The efficiency of the nonlocal beam model to approximate the lattice beam model is shown in presence of rotational elastic link randomness. We also compare such stochastic function with the one of a continuous local Euler–Bernoulli beam, with a special emphasis on scale effect in presence of randomness. Scale effect is captured both in deterministic and non-deterministic frameworks.

Keywords: vibration, lattice elasticity, discrete beams, multibody system dynamics, nonlocal beams.

1. INTRODUCTION

At a microscopic scale, the discontinuous nature of matter may be predominant. However, continuous approximations may be used as a simplification to model the main mechanical phenomenon at a macroscopic level. Periodic structures (see [1, 2]) may be used efficiently to represent discrete microstructures.

Hencky [3] proposed to simulate the behavior of an elastic structure by a finite number of elastically connected rigid segments. The model may be referred to Hencky

bar-chain model. A Hencky bar-chain model comprises rigid bar segments (of length $a = L/n$ where L is the total length of beam and n is the number of segments) connected by elastic rotational springs of stiffness EI/a where EI is the equivalent flexural rigidity of the beam. For this model, the elasticity and the mass of the beam are concentrated at the hinges with rotational springs, as shown in Fig. 1. Hencky bar-chain model could be viewed as a possible discrete model of Euler–Bernoulli beam. Silverman [4] discussed the physical meaning of Henchy bar-chain model and pointed out the mathematical equivalence between the difference equations of Hencky bar-chain model and the Finite Difference Formulation of continuous Euler–Bernoulli beam model for the buckling problem. This equivalence was also shown by Leckie and Lindberg [5] for the vibration problems. Leckie and Lindberg [5] calculated eigenvalues of deterministic lattice beams with different boundary conditions by modeling them by Hencky bar-chain models and other discrete beam models. In their research, they found that the eigenfrequencies of the Hencky bar-chain models depend on the number of segments and converge to the corresponding solutions of the continuous Euler–Bernoulli beam when the number of segments becomes large enough. El Nachie [6] studied the bending and buckling behaviors of Hencky bar-chain models. Zhang et al. [7] discussed the adaptation of Hencky bar-chain to non-uniform beams. Livesley [8] proposed another type of discrete model by supposing that the stiffness may concentrate at the hinges and the

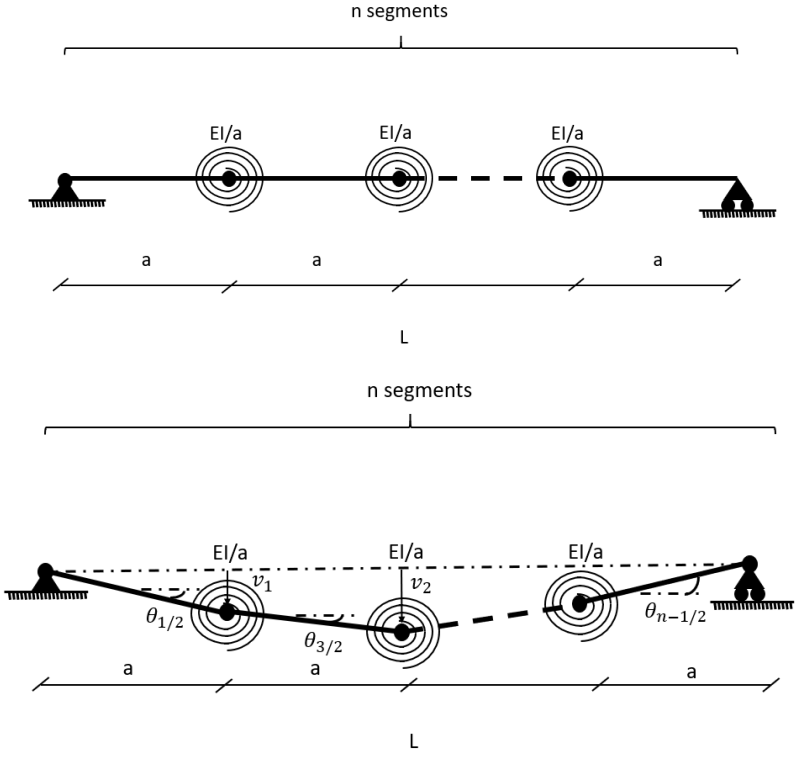

Fig. 1. Simply supported Henchy bar-chain models without and with deformation

mass may distribute along the length of the beam. Leckie and Lindberg [5] also proposed the discrete models with the combinations of concentrated/distributed mass and concentrated/distributed stiffness. In this paper, we will only deal with the Hencky bar-chain model based on concentrated mass and stiffness.

The Finite Difference Method (FDM) is an efficient method to solve continuous problem (see [9,10]). Therefore, Leckie and Lindberg [5] solved a fourth order difference equation applied to the vibration in order to find the eigenfrequencies for lattice beams. Wang et al. [11] discussed about the equivalence between the FDM and the Hencky bar-chain model for several elastic boundary conditions. Exact solutions of vibration equation for lattice beams by FDM in trigonometric and hyperbolic functions are found (see [12–15]). Elishakoff and Santoro (2005) [12] studied the accuracy of FDM for bar elements in a stochastic view. In their study, the stiffness on elastic springs is treated as a continuous random variable, with a given probability density function. Santoro and Elishakoff [13] made a similar study for uniform beam elements. Zhang et al. [15] got analytical solutions of buckling and vibration problems for Hencky bar-chain models with different boundary conditions.

Stochastic mechanics includes some randomness in a mechanical formulation (see [16, 17]). Elishakoff and Soize [16] comprehensively elaborated stochastic models for vibration problems, when there is a random excitation such as earthquake load. Gao et al. [18–20] made the stochastic analysis of beam-type structures and showed the importance of stochastic analysis. There are papers about the stochastic analysis on the Euler–Bernoulli beams (see [21,22]). Silva Junior et al. [22] made a stochastic analysis on Euler–Bernoulli beams by using Askey–Wiener scheme and Galerkin method where the Young modulus is considered as a random variable. Elishakoff and Santoro [12] along with Santoro and Elishakoff [13] studied the performance of the FDM for solving the vibration eigenvalue problems in which the Young modulus is also considered random. They proved that the accuracy of FDM, which is equivalent to the Hencky bar-chain model depends on the number of segments for a stochastic problem.

Nonlocal mechanics captures specific scale effects for repetitive structures which could be used for analysis of micro-structures or large-scale structures such as civil engineering structures. Eringen's nonlocal model (see [23]) used a difference equation to express the relationship between the stress and the strain. Wattis [24] showed how quasi-continuum methods could be used to get approximate solutions of nonlinear differential equations. Andrianov et al. [25] showed that the discrete problem might be analysed by a continuous method based on Padé approximation. Some researchers focused on the scale effects of nonlocal models and found the length scale parameters for lattice models (see [15,26,27]). Duan et al. [26] calculated the length scale parameter from a microstructured Timoshenko element (Timoshenko lattice). Some researchers discuss the adaptation of nonlocal model to different types of problems (see [14, 15, 28, 29]). Reddy [28] discuss the nonlocal theories for bending, buckling and vibration problems for beam models of different beam theories. Challamel et al. [29] and Zhang et al. [15] focused on identifying nonlocal scale parameters for the lattice beams. They discussed the nonlocal scale parameters by comparing the eigenvalues of beams modeling by Eringen's nonlocal model and

Hencky bar-chain model with different boundary conditions for buckling and vibrations problem.

Few works deal with stochastic nonlocal structural models. Potapov [30] analyzed the dynamic stability of Euler–Bernoulli beam based on the nonlocal elasticity theory and nonlocal damping under a stochastic excitation. Alotta et al. [31] introduced a numerical approach to calculate the stochastic response of the nonlocal fractional Timoshenko beam under Gaussian white noise.

In this paper we calculate the eigenvalues by solving in detail the finite difference equations for lattice beams modeling by Hencky bar-chain. There are other approximations for lattice structure such as Myklestad Model [5] with distributed rigidity and concentrated mass but that would be another research. We will study the lattice structure by giving a solution of Hencky bar-chain model based on the finite difference method. Then, the reliabilities of the lattice beams will be determined and compared with those of Euler–Bernoulli beams in a stochastic view. Afterwards, we also calculate the eigenvalues for nonlocal beam approximations as well as their reliabilities. Finally, the accuracies and reliabilities of lattice beams and nonlocal beams will be compared. All these eigenvalues and comparisons are based on scale effect.

2. HENCKY BAR-CHAIN MODEL

Hencky bar-chain model was originally proposed to replace the Euler continuum beam model so that one can obtain solutions by solving a set of algebraic equations instead of a differential equation. Fig. 2 shows part of a uniform beam modeling by Hencky bar-chain model. The length of each segment is a. v_i represents the deflection on the hinge i. The rotation of each segment can be defined in terms of difference of deflection

$$\theta_{i-1/2} = \frac{w_i - w_{i-1}}{a}. \tag{1}$$

The elastic constitutive law for each elastic connection is given by

$$M_i = C*\Delta\theta_i \quad \text{with} \quad C = \frac{EI}{a}. \tag{2}$$

Then the discrete bending moment can be rewritten in terms of deflection

$$M_i = C*\left(\theta_{i+\frac{1}{2}} - \theta_{i-\frac{1}{2}}\right) = C*\frac{w_{i+1} - 2w_i + w_{i-1}}{a} = EI\frac{w_{i+1} - 2w_i + w_{i-1}}{a^2}. \tag{3}$$

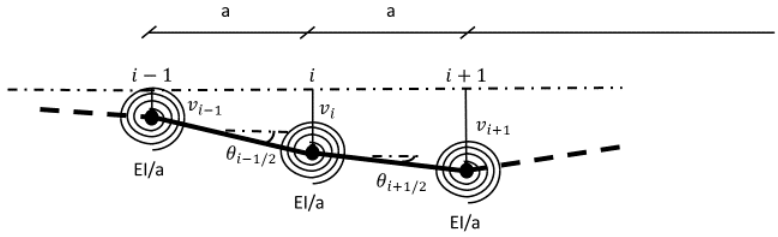

Fig. 2. Basic elements of a uniform Hencky bar-chain beam model with deformation

The equilibrium equation for a Hencky bar-chain model is given by

$$\frac{M_{i+1} - 2M_i + M_{i-1}}{a^2} + \rho A \ddot{w}_i = 0. \tag{4}$$

Eqs. (3) and (4) lead to a fourth order linear difference equation in space. Based on the elastic constitutive law and the equilibrium equation, one gets a mixed differential-difference equation

$$EI\frac{w_{i+2} - 4w_{i+1} + 6w_i - 4w_{i-1} + w_{i-2}}{a^4} + \rho A \ddot{w}_i = 0. \tag{5}$$

Eq. (5) is proposed in [5] and used in [29].

For harmonic motion, the equation of vibration can be expressed as: $w_i = v_i e^{j\omega t}$ with $j^2 = -1$. The free vibration problem is then governed by a linear fourth-order difference equation

$$EI\frac{v_{i+2} - 4v_{i+1} + 6v_i - 4v_{i-1} + v_{i-2}}{a^4} - \rho A \omega^2 v_i = 0. \tag{6}$$

Eq. (6) equivalently corresponds to the finite difference formulation of the vibration of a continuous Euler–Bernoulli beam. With $a = L/n$ and by setting $\Omega^2 = \frac{\rho A \omega^2 L^4}{EI}$, Eq. (6) turns to be

$$v_{i+2} - 4v_{i+1} + 6v_i - 4v_{i-1} + v_{i-2} - \frac{\Omega^2}{n^4} v_i = 0. \tag{7}$$

By setting $v_i = A\lambda^i$, one gets

$$A\lambda^{i+2} - 4A\lambda^{i+1} + (6 - \frac{\Omega^2}{n^4})A\lambda^i - 4A\lambda^{i-1} + A\lambda^{i-2} = 0, \tag{8a}$$

$$(\lambda + \lambda^{-1})^2 - 4(\lambda + \lambda^{-1}) + (4 - \frac{\Omega^2}{n^4}) = 0. \tag{8b}$$

By setting $\lambda + \lambda^{-1} = x$ and $4 - \frac{\Omega^2}{n^4} = b$, Eq. (8b) turns into

$$x^2 - 4x + b = 0, \tag{9}$$

$$x = 2 \pm \sqrt{4 - b}. \tag{10}$$

Retaking $\lambda + \lambda^{-1} = x$, one gets

$$\lambda + \lambda^{-1} = 2 \pm \sqrt{4 - b}, \tag{11}$$

$$\lambda_{1,2} = \frac{2 + \sqrt{4 - b} \pm \sqrt{4 - b + 4\sqrt{4 - b}}}{2}, \tag{12a}$$

$$\lambda_{3,4} = \frac{2 - \sqrt{4 - b} \pm \sqrt{4 - b - 4\sqrt{4 - b}}}{2}. \tag{12b}$$

Bringing back $4-\dfrac{\Omega^2}{n^4}=b$, Eqs. (12) turn to be

$$\lambda_{1,2}=1+\frac{\Omega}{2n^2}\pm\sqrt{(1+\frac{\Omega}{2n^2})^2-1}, \tag{13a}$$

$$\lambda_{3,4}=1-\frac{\Omega}{2n^2}\pm\sqrt{(1-\frac{\Omega}{2n^2})^2-1}. \tag{13b}$$

By setting

$$\cos\phi=1-\frac{\Omega}{2n^2}, \tag{14a}$$

$$\cosh\theta=1+\frac{\Omega}{2n^2}. \tag{14b}$$

v_i can be expressed as

$$v_i=A_1\cos(i\phi)+A_2\sin(i\phi)+A_3\cosh(i\theta)+A_4\sinh(i\theta). \tag{15}$$

Eq. (15) has been formulated in [5] and practiced in [14,15,32].

2.1. For simply supported-simply supported beam

The boundary conditions of a simply supported-simply supported lattice beam are

$$\begin{cases} v_0=0 \\ v_n=0 \\ M_0=0\Rightarrow v_{-1}=-v_1 \\ M_n=0\Rightarrow v_{n-1}=-v_{n+1} \end{cases} \tag{16}$$

Coupling Eq. (15) with Eq. (16) and setting the determinant of homogeneous coefficient matrix to zero in order to make the expression of v_i meaningful, one gets the following determinant

$$\begin{bmatrix} 1 & 0 & 1 & 0 \\ \cos(n\phi) & \sin(n\phi) & \cosh(n\theta) & \sinh(n\theta) \\ 2\cos\phi & 0 & 2\cosh\theta & 0 \\ 2\cos\phi\cos(n\phi) & 2\cos\phi\sin(n\phi) & 2\cosh\theta\cosh(n\theta) & 2\cosh\theta\sinh(n\theta) \end{bmatrix}=0. \tag{17}$$

Eq. (17) can be simplified and solved

$$4\sin(n\phi)\sinh(n\theta)(\cosh\theta-\cos\phi)^2=0, \tag{18a}$$

$$\sin(n\phi)=0 \quad \text{or} \quad \sinh(n\theta)=0 \quad \text{or} \quad \cosh\theta-\cos\phi=0. \tag{18b}$$

Therefore

$$n\phi=k\pi \quad \text{or} \quad n\theta=0 \quad \text{or} \quad \cosh\theta=\cos\phi. \tag{19}$$

With Eqs. (14a) above, only $n\phi=k\pi$ leads to a non-trivial solution. Ω can be expressed as

$$\cos\left(\frac{k\pi}{n}\right)=1-\frac{\Omega}{2n^2}, \tag{20a}$$

$$\Omega=4n^2\sin^2\left(\frac{k\pi}{2n}\right), \tag{20b}$$

which has been obtained as well by Leckie and Lindberg [5]. With $\Omega^2 = \dfrac{\rho A \omega^2 L^4}{EI}$, one obtains the eigen circular frequency

$$\omega = \frac{4n^2 \sin^2\left(\frac{k\pi}{2n}\right)}{L^2}\sqrt{\frac{EI}{\rho A}} \quad \text{with} \quad k = 1, 2, 3 \ldots \tag{21}$$

One finds that the eigen circular frequency of each mode is a function of the number of segments n. When n approaches infinity, Eq. (21) turns to be

$$\omega = \left(\frac{k\pi}{L}\right)^2 \sqrt{\frac{EI}{\rho A}} \quad \text{with} \quad k = 1, 2, 3 \ldots \tag{22}$$

Eq. (22) coincides with the frequency of a continuous simply supported-simply supported Euler–Bernoulli beam given in [33].

As the first eigenfrequency is usually the most important for a structure, k is set to 1 which corresponds to the first mode. With the increase of n, the value of Ω_1 of the first mode as a representative mode when $k = 1$ can be seen in Fig. 3. In the paper, the results are mainly based on the first mode. By setting $k = 2, 3, \ldots$, one can get the results based on the second, the third mode, etc. When n equals to 20, $\Omega_1 = 9.8513$ is close to that of a continuous Euler–Bernoulli beam whose $\Omega_{1,\infty} = \pi^2 = 9.8696$ given in [32, 33].

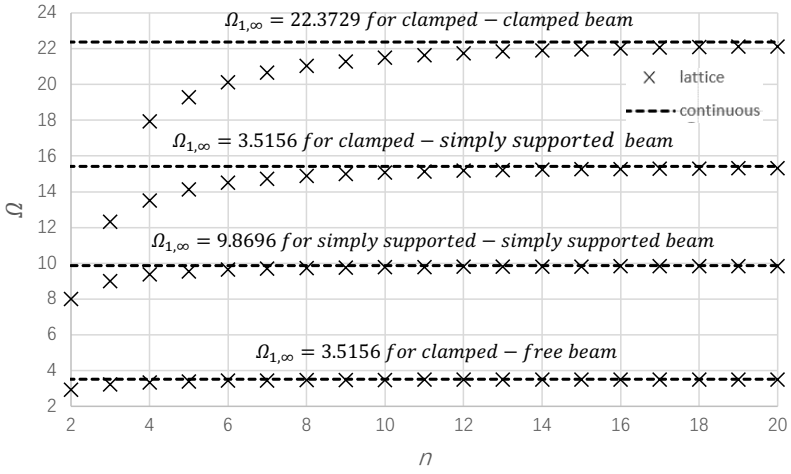

Fig. 3. Eigen value Ω_1 of the first mode with an increase of n for lattice beams of simply supported-simply supported/clamped-clamped/clamped-free/simply supported-clamped

2.2. For clamped-clamped beam

The boundary conditions of a clamped-clamped lattice beam are

$$\begin{cases} v_0 = 0 \\ v_n = 0 \\ \theta_{\frac{1}{2}} + \theta_{-\frac{1}{2}} = 0 \Rightarrow v_{-1} = v_1 \\ \theta_{n+\frac{1}{2}} + \theta_{n-\frac{1}{2}} = 0 \Rightarrow v_{n-1} = v_{n+1} \end{cases} \tag{23}$$

Coupling Eq. (15) with Eq. (23) and setting the determinant of homogeneous coefficient matrix to zero in order to make the expression of v_i meaningful, one gets

$$\begin{bmatrix} 1 & 0 & 1 & 0 \\ \cos(n\phi) & \sin(n\phi) & \cosh(n\theta) & \sinh(n\theta) \\ 0 & 2\sin\phi & 0 & 2\sinh\theta \\ -2\sin\phi\sin(n\phi) & 2\sin\phi\cos(n\phi) & 2\sinh\theta\sinh(n\theta) & 2\sinh\theta\cosh(n\theta) \end{bmatrix} = 0. \tag{24}$$

Eq. (**??**) can be simplified as

$$[2 - 2\cos(n\phi)\cosh(n\theta)]\sin\phi\sinh\theta + \left(\sinh^2\theta - \sin^2\phi\right)\sinh(n\theta)\sin(n\phi) = 0. \tag{25}$$

For comparison, we practice the method in [5] by setting the origin point on the middle of the beam for the number of segments n, the boundary conditions change to

$$\begin{cases} v_{\frac{n}{2}} = 0 \\ v_{-\frac{n}{2}} = 0 \\ \theta_{-\frac{n}{2}+\frac{1}{2}} + \theta_{-\frac{n}{2}-\frac{1}{2}} = 0 \Rightarrow v_{-\frac{n}{2}-1} = v_{-\frac{n}{2}+1} \\ \theta_{\frac{n}{2}+\frac{1}{2}} + \theta_{\frac{n}{2}-\frac{1}{2}} = 0 \Rightarrow v_{\frac{n}{2}-1} = v_{\frac{n}{2}+1} \end{cases} \tag{26}$$

If one considers only the symmetrical vibration modes about the origin point, Eq. (15) can be simplified as

$$v_i = A_1\cos(i\phi) + A_3\cosh(i\theta). \tag{27}$$

Coupling Eq. (26) with Eq. (27) and setting the determinant of homogeneous coefficient matrix to zero in order to make the expression of v_i meaningful, one gets

$$\begin{bmatrix} \cos\left(\frac{n\phi}{2}\right) & \cosh\left(\frac{n\theta}{2}\right) \\ 2\sin\phi\sin\left(\frac{n\phi}{2}\right) & -2\sinh\theta\sinh\left(\frac{n\theta}{2}\right) \end{bmatrix} = 0. \tag{28}$$

Eq. (28) can be simplified as

$$\sinh\theta * \tanh\left(\frac{n\theta}{2}\right) + \sin\phi * \tan\left(\frac{n\phi}{2}\right) = 0, \tag{29}$$

which is obtained by Leckie and Lindberg [5] with $2n$ elements instead of n elements considered in this paper. Simultaneously, Eq. (25) can be changed to

$$\left[\sinh\theta\tanh\left(\frac{n\theta}{2}\right) + \sin\phi\tan\left(\frac{n\phi}{2}\right)\right] * \left[\tan\left(\frac{n\phi}{2}\right)\sinh\theta - \tanh\left(\frac{n\theta}{2}\right)\sin\phi\right] = 0. \tag{30}$$

One notices that the first part of the left side of Eq. (30) coincides with Eq. (29). In fact, the first part of the left side of Eq. (30) describes the characteristic of the symmetrical modes and the second part describes the characteristic of the asymmetric modes. By coupling Eqs. (14) with Eq. (30), one can find the Ω value by a function of k and n.

With the increase of n, the value of Ω_1 of the first mode when $k = 1$ can be seen in Fig. 3. When n equals to 20, $\Omega_1 = 22.2907$ is close to that of a continuous Euler–Bernoulli beam whose $\Omega_{1,\infty} = 22.3729$ given in [32,33].

2.3. For clamped-free beam

For a clamped-free beam, considering that at the end $i = 0$ of the beam is clamped and at the end $i = n$ is free, the boundary conditions are

$$\begin{cases} v_0 = 0 \\ \theta_{\frac{1}{2}} + \theta_{-\frac{1}{2}} = 0 \Rightarrow v_{-1} = v_1 \\ M_n = 0 \Rightarrow v_{n+1} - 2v_n + v_{n-1} = 0 \\ M_{n+1} - M_{n-1} = 0 \Rightarrow v_{n+2} - 2v_{n+1} + 2v_{n-1} - v_{n-2} = 0 \end{cases} \tag{31}$$

Coupling Eq. (15) with Eq. (31) and setting the determinant of homogeneous coefficient matrix to zero in order to make the expression of v_i meaningful, one gets

$$\begin{bmatrix} 1 & 0 & 1 & 0 \\ 0 & 2\sin\phi & 0 & 2\sinh\theta \\ 2\cos(n\phi)(\cos\phi - 1) & 2\sin(n\phi)(\cos\phi - 1) & 2\cosh(n\theta)(\cosh\theta - 1) & 2\sinh(n\theta)(\cosh\theta - 1) \\ F_1 & F_2 & F_3 & F_4 \end{bmatrix} = 0,$$

$$\begin{aligned} F_1 &= 4\sin\phi\sin(n\phi)(1 - \cos\phi), \\ F_2 &= 4\sin\phi\cos(n\phi)(\cos\phi - 1), \\ F_3 &= 4\sinh\theta\sinh(n\theta)(\cosh\theta - 1), \\ F_4 &= 4\sinh\theta\cosh(n\theta)(\cosh\theta - 1). \end{aligned} \tag{32}$$

By coupling Eqs. (14) with Eq. (32), one can find the Ω value by a function of k and n.

With the increase of n, the value of Ω_1 of the first mode when $k = 1$ can be seen in Fig. 3. When n equals to 20, $\Omega_1 = 3.5066$ is close to the that of a continuous Euler–Bernoulli beam whose $\Omega_{1,\infty} = 3.5156$ given in [33].

2.4. For clamped-simply supported beam

For a clamped-simply supported beam, considering that at the end $i = 0$ of the beam is clamped and at the end $i = n$ is simply supported, the boundary conditions are

$$\begin{cases} v_0 = 0 \\ v_n = 0 \\ \theta_{\frac{1}{2}} + \theta_{-\frac{1}{2}} = 0 \Rightarrow v_{-1} = v_1 \\ M_n = 0 \Rightarrow v_{n-1} = -v_{n+1} \end{cases} \tag{33}$$

Coupling Eq. (15) with Eq. (33) and setting the determinant of homogeneous coefficient matrix to zero in order to make the expression of v_i meaningful, one gets

$$\begin{bmatrix} 1 & 0 & 1 & 0 \\ \cos(n\phi) & \sin(n\phi) & \cosh(n\theta) & \sinh(n\theta) \\ 0 & 2\sin\phi & 0 & 2\sinh\theta \\ 2\cos\phi\cos(n\phi) & 2\cos\phi\sin(n\phi) & 2\cosh\theta\cosh(n\theta) & 2\cosh\theta\sinh(n\theta) \end{bmatrix} = 0. \tag{34}$$

Eq. (34) can be simplified as

$$(\cos\phi - \cosh\theta)\left[\sin\phi\cos(n\phi)\sinh(n\theta) - \sinh\theta\sin(n\phi)\cosh(n\theta)\right] = 0. \tag{35}$$

By coupling Eqs. (14) with Eq. (35), one can find the Ω value by a function of k and n.

With the increase of n, the value of Ω_1 of the first mode when $k = 1$ can be seen in Fig. 3. When n equals to 20, $\Omega_1 = 15.3437$ is close to the that of a continuous Euler–Bernoulli beam whose $\Omega_{1,\infty} = 15.4182$ given in [33]. Exact formula of eigenfrequencies of Hencky-chain bar under various boundary conditions (including the hinge-hinge, clamped-free, clamped-clamped and clamped-hinge boundary conditions) are available in Wang et al. (2017) [34] and in Wang et al. (2020) [35].

3. STOCHASTIC ANALYSIS OF THE LATTICE BEAMS

The purpose to get the eigenfrequency is to avoid the resonance. The circular eigenfrequency of the first mode ω_1 should be less than an excitation circular frequency ω_0.

$$\omega_1 < \omega_0. \tag{36}$$

In the stochastic analysis, each of the stiffness of elastic links between the segments is treated as a continuous random variable. As the fundamental eigenfrequency is a function of the stiffness, it also turns out to be a random variable.

3.1. For simply supported-simply supported beam

Based on Eq. (22), the circular eigenfrequency of the first mode is

$$\omega_1 = \frac{4n^2\sin^2\left(\frac{\pi}{2n}\right)}{L^2}\sqrt{\frac{EI}{\rho A}} = \frac{\pi^2}{L^2}\sqrt{\frac{EI}{\rho A}}\frac{\sin^2\left(\frac{\pi}{2n}\right)}{\left(\frac{\pi}{2n}\right)^2}. \tag{37}$$

The reliability R (see [36]) of the beam can be defined as the probability that the square of this fundamental frequency is less than the square of an excitation frequency

$$R = Prob\left[\left(\frac{\pi^2}{L^2}\sqrt{\frac{EI}{\rho A}}\frac{\sin^2\left(\frac{\pi}{2n}\right)}{\left(\frac{\pi}{2n}\right)^2}\right)^2 < {\omega_0}^2\right] = Prob\left[EI < \frac{{\omega_0}^2L^4\rho A}{\pi^4}\frac{\left(\frac{\pi}{2n}\right)^4}{\sin^4\left(\frac{\pi}{2n}\right)}\right], \tag{38a}$$

$$R = F_{EI}\left[\frac{{\omega_0}^2L^4\rho A}{\pi^4}\frac{\left(\frac{\pi}{2n}\right)^4}{\sin^4\left(\frac{\pi}{2n}\right)}\right], \tag{38b}$$

where F_{EI} is the probability distribution function of EI.

Consider the case when the random variable of Young's modulus is modelling as an exponential distribution since exponential distribution is mainly used for the case of failure. The density function of this exponential distribution is given by

$$f(EI) = \begin{cases} 0 & EI < 0 \\ \mu e^{-\mu EI} & EI \geq 0, \mu > 0 \end{cases} \tag{39}$$

with the expectation $M[EI] = 1/\mu$ and the variance $Var[EI] = 1/\mu^2$. The distribution function is given by

$$F(EI) = \begin{cases} 0 & EI < 0 \\ 1 - \exp(-\mu EI) & EI \geq 0, \mu > 0 \end{cases} \tag{40}$$

where

$$Prob\{EI \leq x\} = 1 - \exp\left(-\frac{x}{M[EI]}\right). \tag{41}$$

Coupling Eq. (40) with Eq. (38a) and Eq. (38b), the expression of the reliability for a lattice beam is

$$R_{lattice} = 1 - exp\left[-\frac{1}{M[EI]}\frac{{\omega_0}^2 L^4 \rho A}{\pi^4}\frac{\left(\frac{\pi}{2n}\right)^4}{\sin^4\left(\frac{\pi}{2n}\right)}\right]. \tag{42}$$

In order to learn the scale effect based on n, we compare such stochastic reliability with that of a continuous local Euler–Bernoulli beam. For a simply supported-simply supported continuous local Euler–Bernoulli beam, the reliability in this case is

$$R_{local} = Prob\left[\frac{\pi^4}{L^4}\frac{EI}{\rho A} < {\omega_0}^2\right] = 1 - exp\left[-\frac{1}{M[EI]}\frac{{\omega_0}^2 L^4 \rho A}{\pi^4}\right]. \tag{43}$$

Coupling Eq. (42) and Eq. (43), one finds that the only difference between $R_{lattice}$ and R_{local} is the factor $\frac{\left(\frac{\pi}{2n}\right)^4}{\sin^4\left(\frac{\pi}{2n}\right)}$. By setting $R_{local} = r_0$ where r_0 is the codified reliability value, the relationship between $R_{lattice}$ and r_0 is

$$1 - R_{lattice} = \exp\left[-\frac{1}{M[EI]}\frac{{\omega_0}^2 L^4 \rho A}{\pi^4}\frac{\left(\frac{\pi}{2n}\right)^4}{\sin^4\left(\frac{\pi}{2n}\right)}\right] = (1 - R_{local})^{\left[\frac{\frac{\pi}{2n}}{\sin\left(\frac{\pi}{2n}\right)}\right]^4}, \tag{44a}$$

$$R_{lattice} = 1 - (1 - r_0)^{\left[\frac{\frac{\pi}{2n}}{\sin\left(\frac{\pi}{2n}\right)}\right]^4}. \tag{44b}$$

The probability of failure is conceptually opposite to the reliability

$$P_{lattice} = 1 - R_{lattice}, \tag{45a}$$

$$p_0 = 1 - R_{local} = 1 - r_0. \tag{45b}$$

By combining Eq. (44b) along with Eq. (45a) and Eq. (45b), the relationship between $P_{lattice}$ and p_0 is

$$P_{lattice} = 1 - R_{lattice} = (1 - r_0)^{\left[\frac{\frac{\pi}{2n}}{\sin\left(\frac{\pi}{2n}\right)}\right]^4} = p_0^{\left[\frac{\frac{\pi}{2n}}{\sin\left(\frac{\pi}{2n}\right)}\right]^4}. \tag{46}$$

The ratio of $P_{lattice}$ to p_0 can be expressed as a function of n

$$\frac{P_{lattice}}{p_0} = \frac{p_0^{\left[\frac{\frac{\pi}{2n}}{\sin\left(\frac{\pi}{2n}\right)}\right]^4}}{p_0} = p_0^{\left[\frac{\frac{\pi}{2n}}{\sin\left(\frac{\pi}{2n}\right)}\right]^4 - 1}. \tag{47}$$

Variation of $P_{lattice}$, as a function of n, when p_0 fixed at 0.1, 0.01 and 0.001, is portrayed in Fig. 4. The values of $P_{lattice}/p_0$ can be seen in Fig. 5.

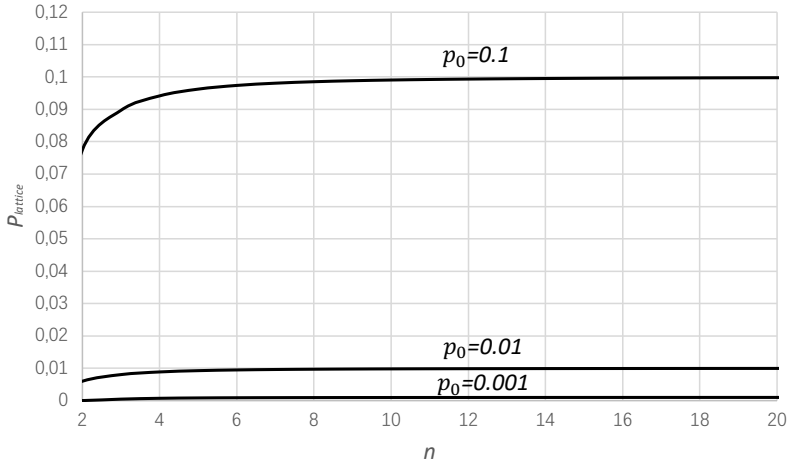

Fig. 4. Probability of failure of a simply supported-simply supported lattice beam with an increasing n when the probability of failure of a corresponding simply supported-simply supported Euler–Bernoulli beam $p_0 \in \{0.1,\ 0.01,\ 0.001\}$

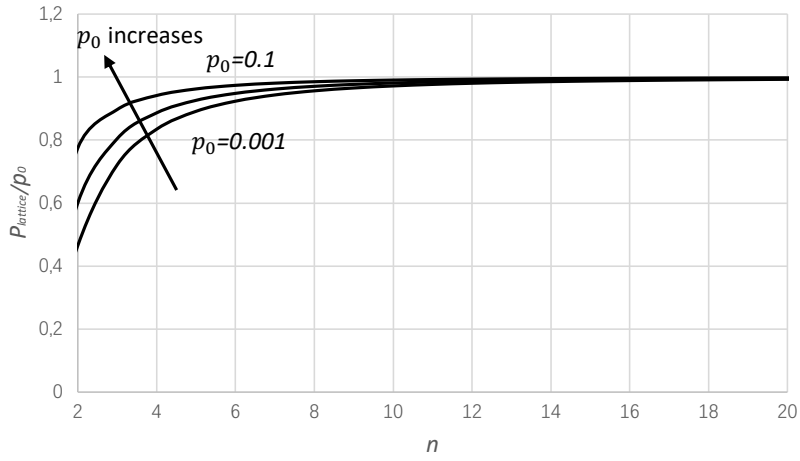

Fig. 5. Ratio of probability of failure of simply supported-simply supported lattice beam to probability of failure of a corresponding simply supported-simply supported Euler–Bernoulli beam $p_0 \in \{0.1,\ 0.01,\ 0.001\}$

3.2. For clamped-clamped beam

With $\Omega^2 = \dfrac{\rho A \omega^2 L^4}{EI}$, the circular eigenfrequency of the first mode is

$$\omega_1 = \frac{\Omega_1(n)}{L^2}\sqrt{\frac{EI}{\rho A}}. \tag{48}$$

Similar to the case of simply supported-simply supported beam, the reliability R can be defined as the probability that the square of the fundamental frequency is less than the square of an excitation frequency

$$R = Prob\left[\left(\frac{\Omega_1(n)}{L^2}\sqrt{\frac{EI}{\rho A}}\right)^2 < {\omega_0}^2\right] = Prob\left[EI < \frac{{\omega_0}^2 L^4 \rho A}{\Omega_1^2(n)}\right] = F_{EI}\left[\frac{{\omega_0}^2 L^4 \rho A}{\Omega_1^2(n)}\right]. \tag{49}$$

Coupling Eq. (41) with Eq. (49), the expression of the reliability for a lattice beam is

$$R_{lattice} = 1 - \exp\left[-\frac{1}{M[EI]}\frac{{\omega_0}^2 L^4 \rho A}{\Omega_1^2(n)}\right]. \tag{50}$$

For a clamped-clamped continuous local Euler–Bernoulli beam, the reliability in this case is

$$R_{local} = Prob\left[\frac{{\Omega^2}_{1,\infty}}{L^4}\frac{EI}{\rho A} < {\omega_0}^2\right], \tag{51a}$$

$$R_{local} = 1 - \exp\left[-\frac{1}{M[EI]}\frac{{\omega_0}^2 L^4 \rho A}{{\Omega^2}_{1,\infty}}\right]. \tag{51b}$$

With the equation of $\Omega_{1,\infty}$ which is given in [33]

$$\cos\left(\sqrt{\Omega_{1,\infty}}\right)\cosh\left(\sqrt{\Omega_{1,\infty}}\right) = 1, \tag{52a}$$

$$\sqrt{\Omega_{1,\infty}} = 4.7300. \tag{52b}$$

By setting $R_{local} = r_0$ where r_0 is the codified reliability value, the relationship between $R_{lattice}$ and r_0 is

$$1 - R_{lattice} = \exp\left[-\frac{1}{M[EI]}\frac{{\omega_0}^2 L^4 \rho A}{\Omega_1^2(n)}\right] = (1 - R_{local})^{\frac{\Omega_{1,\infty}^2}{\Omega_1^2(n)}}, \tag{53a}$$

$$R_{lattice} = 1 - (1 - r_0)^{\frac{\Omega_{1,\infty}^2}{\Omega_1^2(n)}}. \tag{53b}$$

By coupling Eq. (53b) along with Eq. (45a) and Eq. (45b), the relationship between $P_{lattice}$ and p_0 is

$$P_{lattice} = 1 - R_{lattice} = (1 - r_0)^{\frac{\Omega_{1,\infty}^2}{\Omega_1^2(n)}} = {p_0}^{\frac{\Omega_{1,\infty}^2}{\Omega_1^2(n)}}. \tag{54}$$

The ratio of $P_{lattice}$ to p_0 could be expressed as a function of n

$$\frac{P_{lattice}}{p_0} = \frac{{p_0}^{\frac{\Omega_{1,\infty}^2}{\Omega_1^2(n)}}}{p_0} = {p_0}^{\frac{\Omega_{1,\infty}^2}{\Omega_1^2(n)} - 1}. \tag{55}$$

With the increase of n, when p_0 equals to 0.1, 0.01 and 0.001, the values of $P_{lattice}$ can be seen in Fig. 6. The values of $P_{lattice}/p_0$ can be seen in Fig. 7.

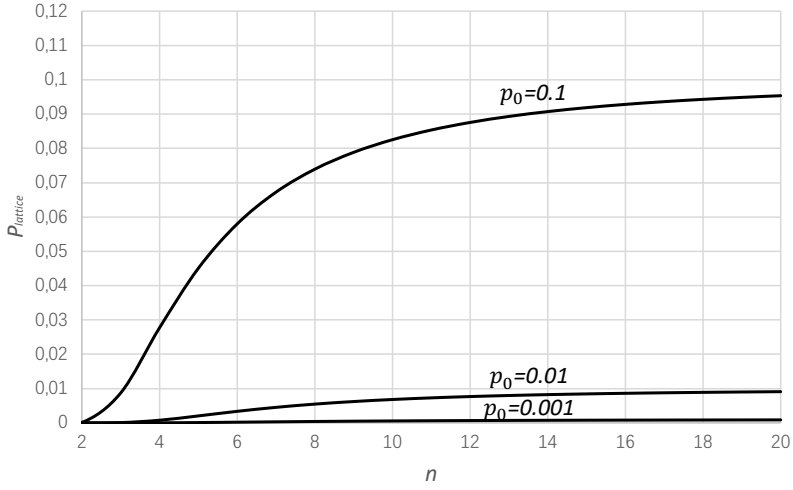

Fig. 6. Probability of failure of a clamped-clamped lattice beam with an increasing n when the probability of failure of a corresponding clamped-clamped Euler–Bernoulli beam $p_0 \in \{0.1,\ 0.01,\ 0.001\}$

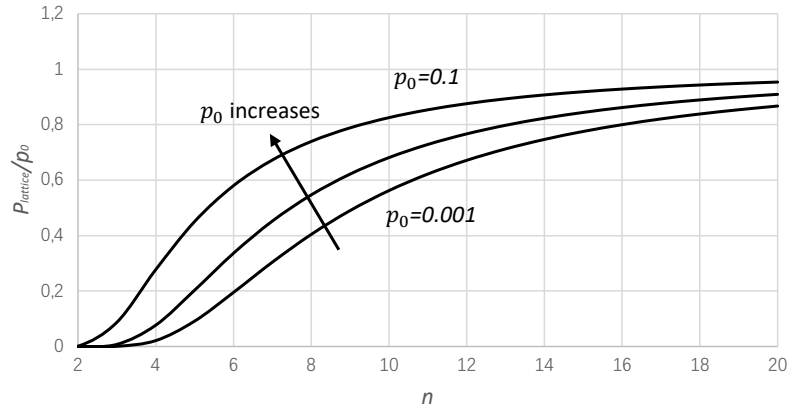

Fig. 7. Ratio of probability of failure of clamped-clamped lattice beam to probability of failure of a corresponding clamped-clamped Euler–Bernoulli beam $p_0 \in \{0.1,\ 0.01,\ 0.001\}$

3.3. For clamped-free beam

For a clamped-free beam, the relationship between $P_{lattice}$ and p_0 is also given by Eq. (45a) and Eq. (45b), with the equation of $\Omega_{1,\infty}$ given in [33]

$$\cos\left(\sqrt{\Omega_{1,\infty}}\right)\cosh\left(\sqrt{\Omega_{1,\infty}}\right)+1=0, \tag{56a}$$

$$\sqrt{\Omega_{1,\infty}} = 1.8751. \tag{56b}$$

With the increase of n, when p_0 equals to 0.1, 0.01 and 0.001, the values of $P_{lattice}$ can be seen in Fig. 8. The values of $P_{lattice}/p_0$ can be seen in Fig. 9.

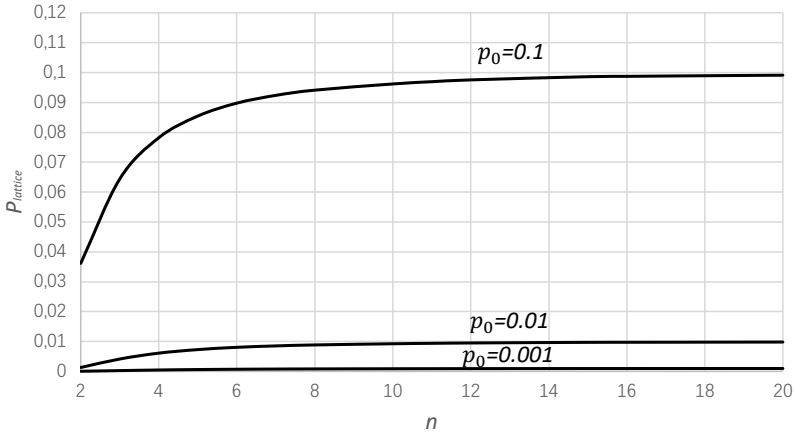

Fig. 8. Probability of failure of a clamped-free lattice beam with an increasing n when the probability of failure of a corresponding clamped-free Euler–Bernoulli beam $p_0 \in \{0.1,\ 0.01,\ 0.001\}$

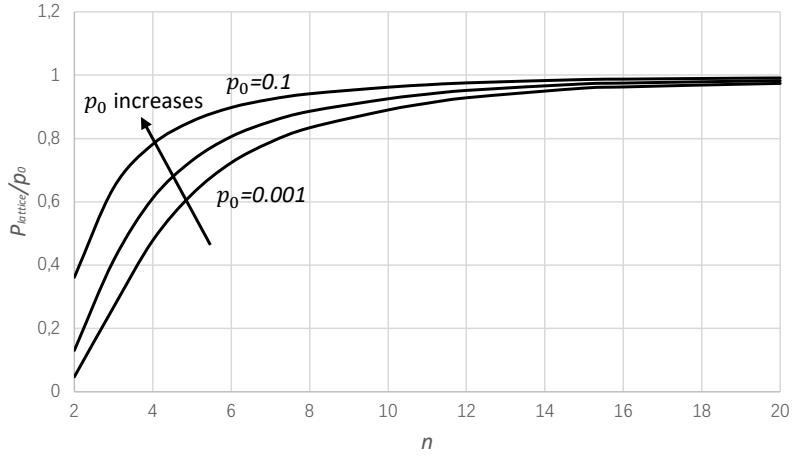

Fig. 9. Ratio of probability of failure of clamped-free lattice beam to probability of failure of a corresponding clamped-free Euler–Bernoulli beam $p_0 \in \{0.1,\ 0.01,\ 0.001\}$

3.4. For clamped-simply supported beam

For a clamped-free beam, the relationship between $P_{lattice}$ and p_0 is also given by Eq. (45a) and Eq. (45b), with the equation of $\Omega_{1,\infty}$ given in [33]

$$\sin\left(\sqrt{\Omega_{1,\infty}}\right)\cosh\left(\sqrt{\Omega_{1,\infty}}\right) - \cos\left(\sqrt{\Omega_{1,\infty}}\right)\sinh\left(\sqrt{\Omega_{1,\infty}}\right) = 0, \tag{57a}$$

$$\sqrt{\Omega_{1,\infty}} = 3.9266. \tag{57b}$$

With the increase of n, when p_0 equals to 0.1, 0.01 and 0.001, the values of $P_{lattice}$ can be seen in Fig. 10. The values of $P_{lattice}/p_0$ can be seen in Fig. 11.

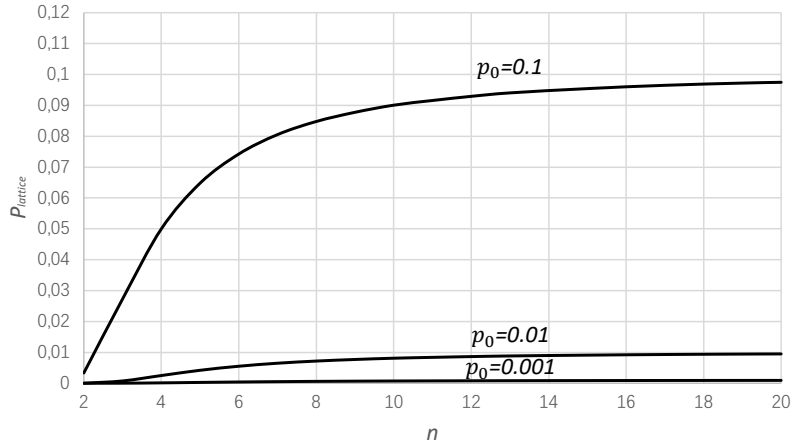

Fig. 10. Probability of failure of a clamped-simply supported lattice beam with an increasing n when the probability of failure of a corresponding clamped-simply supported Euler–Bernoulli beam $p_0 \in \{0.1,\ 0.01,\ 0.001\}$

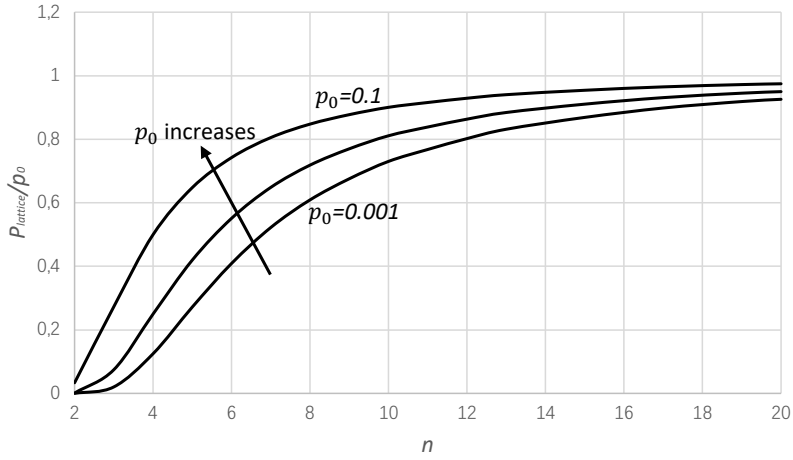

Fig. 11. Ratio of probability of failure of clamped-simply supported lattice beam to probability of failure of a corresponding clamped-simply supported Euler–Bernoulli beam $p_0 \in \{0.1,\ 0.01,\ 0.001\}$

4. NONLOCAL BEAM MECHANICS

Eq. (3) is the finite difference equation for a continuous Euler–Bernoulli beam. Hence the discrete micro-structured system is mathematically equivalent to the finite difference

format of the so-called "local" continuous system. The discrete equation is extended to an equivalent continuous one via a "continualization" method. The relationship between the discrete system and the equivalent continuous system $v_i = v(x = ia)$ has a sufficiently smooth deflection function as

$$w(x+a) = w(x) + aw'(x) + \frac{a^2}{2}w''(x) + \frac{a^3}{6}w'''(x) + \ldots = \sum_{k=0}^{\infty} \frac{a^k \partial_x^k}{k!} w(x) = e^{a\partial_x} w(x). \tag{58}$$

Eq. (58) can be expressed as

$$w(x+a) = e^{a\partial_x} w(x). \tag{59}$$

The pseudo-differential operators may be introduced

$$w_{i+1} - 2w_i + w_{i-1} = \left(e^{a\partial_x} + e^{-a\partial_x} - 2\right) w(x) = 4\sinh^2\left(\frac{a\partial_x}{2}\right) w(x), \tag{60a}$$

$$\begin{aligned} w_{i+2} - 4w_{i+1} + 6w_i - 4w_{i-1} + w_{i-2} &= \left(e^{2a\partial_x} - 4e^{a\partial_x} + 6 - 4e^{-a\partial_x} + e^{-2a\partial_x}\right) w(x) \\ &= \left(e^{a\partial_x} + e^{-a\partial_x} - 2\right)^2 w(x) \\ &= 16\sinh^4\left(\frac{a\partial_x}{2}\right) w(x). \end{aligned} \tag{60b}$$

Coupling with Eq. (60b), Eq. (3) is reexpressed as

$$\frac{16EI\sinh^4\left(\frac{a\partial_x}{2}\right)}{a^4} w + \rho A\ddot{w} = 0. \tag{61}$$

It is possible to approximate the pseudo-differential operators through Padé's approximation

$$\frac{4\sinh^2\left(\frac{a\partial_x}{2}\right)}{a^2} = \frac{12{\partial_x}^2}{-(a\partial_x)^2 + 12} = \frac{{\partial_x}^2}{1 - l_c{}^2{\partial_x}^2} + \ldots \quad \text{with} \quad l_c{}^2 = \frac{a^2}{12}. \tag{62}$$

Eq. (62) has been practiced in [37]. With Eqs. (62), (61) can be approximated by the linear differential equation

$$EI\left(\frac{{\partial_x}^2}{1 - l_c{}^2{\partial_x}^2}\right)^2 w + \rho A\ddot{w} = 0, \tag{63a}$$

$$EI{\partial_x}^4 w + \rho A{\partial_t}^2(1 - 2l_c{}^2{\partial_x}^2 + l_c{}^4{\partial_x}^4)w = 0. \tag{63b}$$

As the part of partial derivatives of six order can be ignored, Eq. (63b) turns to be

$$EI{\partial_x}^4 w + \rho A{\partial_t}^2\left(1 - 2l_c{}^2{\partial_x}^2\right) w = 0. \tag{64}$$

For harmonic motion, $w(x,t) = v(x)e^{j\omega t}$ with $j^2 = -1$, Eq. (64) turns into

$$EI{\partial_x}^4 v + \rho A\omega^2\left(2l_c{}^2{\partial_x}^2 - 1\right) v = 0. \tag{65}$$

Adopting the non-dimensional terms

$$\overline{v} = \frac{v}{L}, \quad \overline{x} = \frac{x}{L}, \quad \Omega^2 = \frac{\rho A \omega^2 L^4}{EI}. \tag{66}$$

With Eqs. (66), (65) turns to be

$$\partial_{\overline{x}}{}^4 \overline{v} + \frac{2{l_c}^2 \Omega^2}{L^2} \partial_{\overline{x}}{}^2 \overline{v} - \Omega^2 \overline{v} = 0. \tag{67}$$

The characteristic equation of Eq. (67) is given

$$r^4 + \frac{2{l_c}^2 \Omega^2}{L^2} r^2 - \Omega^2 = 0, \tag{68}$$

with ${l_c}^2 = \dfrac{a^2}{12}$

$$r^2 = -\frac{\Omega^2}{12n^2} \pm \sqrt{\left(\frac{\Omega^2}{12n^2}\right)^2 + \Omega^2}. \tag{69}$$

The roots r of the characteristic equation are given by

$$r_{1,2} = \pm \sqrt{-\frac{\Omega^2}{12n^2} + \sqrt{\left(\frac{\Omega^2}{12n^2}\right)^2 + \Omega^2}}, \tag{70a}$$

$$r_{3,4} = \pm j \sqrt{\frac{\Omega^2}{12n^2} + \sqrt{\left(\frac{\Omega^2}{12n^2}\right)^2 + \Omega^2}} \quad \text{with} \quad j^2 = -1. \tag{70b}$$

The general solution of Eq. (67) is

$$\overline{v}\left(\overline{x}\right) = D_1 \cos(\beta \overline{x}) + D_2 \sin\left(\beta \overline{x}\right) + D_3 \cosh\left(\eta \overline{x}\right) + D_4 \sinh\left(\eta \overline{x}\right), \tag{71a}$$

$$\beta = \sqrt{\frac{\Omega^2}{12n^2} + \sqrt{\left(\frac{\Omega^2}{12n^2}\right)^2 + \Omega^2}}, \tag{71b}$$

with

$$\eta = \sqrt{-\frac{\Omega^2}{12n^2} + \sqrt{\left(\frac{\Omega^2}{12n^2}\right)^2 + \Omega^2}}. \tag{71c}$$

4.1. For simply supported-simply supported beam

The mode shape of a simply supported-simply supported beam is a sinusoidal form given by

$$v = v_0 \sin\left(\frac{k\pi x}{L}\right). \tag{72}$$

By coupling Eq. (67) and Eq. (72), one gets

$$EI\left(\frac{k\pi}{L}\right)^4 v_0 \sin\left(\frac{k\pi x}{L}\right) - 2\rho A \omega^2 {l_c}^2 \left(\frac{k\pi}{L}\right)^2 v_0 \sin\left(\frac{k\pi x}{L}\right) - \rho A \omega^2 v_0 \sin\left(\frac{k\pi x}{L}\right) = 0, \tag{73a}$$

$$EI\left(\frac{k\pi}{L}\right)^4 - 2\rho A\omega^2 {l_c}^2\left(\frac{k\pi}{L}\right)^2 - \rho A\omega^2 = 0. \tag{73b}$$

The eigen circular frequency is

$$\omega^2 = \frac{EI\left(\frac{k\pi}{L}\right)^4}{\rho A\left[2{l_c}^2\left(\frac{k\pi}{L}\right)^2 + 1\right]}, \tag{74}$$

with ${l_c}^2 = \dfrac{a^2}{12}$, one obtains

$$\omega^2 = \frac{EI\left(\frac{k\pi}{L}\right)^4}{\rho A\left[\frac{a^2}{6}\left(\frac{k\pi}{L}\right)^2 + 1\right]} = \frac{EI\left(\frac{k\pi}{L}\right)^4}{\rho A\left[\frac{1}{6}\left(\frac{k\pi}{n}\right)^2 + 1\right]}. \tag{75}$$

This result can be found again from the following non-dimensional boundary conditions, expressed as

$$\begin{cases} \overline{v}(0) = 0 \\ \overline{v}(1) = 0 \\ \overline{M}(0) = 0 \Rightarrow \overline{v}\left(\dfrac{1}{n}\right) + \overline{v}\left(-\dfrac{1}{n}\right) = 0 \\ \overline{M}(1) = 0 \Rightarrow \overline{v}\left(1 + \dfrac{1}{n}\right) + \overline{v}\left(1 - \dfrac{1}{n}\right) = 0 \end{cases} \tag{76}$$

Coupling Eq. (71a) with Eq. (76) and setting the determinant of homogeneous coefficient matrix to zero in order to make the expression of v_i meaningful, one gets

$$\begin{bmatrix} 1 & 0 & 1 & 0 \\ \cos(\beta) & \sin(\beta) & \cosh(\eta) & \sinh(\eta) \\ 2\cos\left(\dfrac{\beta}{n}\right) & 0 & 2\cosh\left(\dfrac{\eta}{n}\right) & 0 \\ 2\cos(\beta)\cos\left(\dfrac{\beta}{n}\right) & 2\sin(\beta)\cos\left(\dfrac{\beta}{n}\right) & 2\cosh(\eta)\cosh\left(\dfrac{\eta}{n}\right) & 2\sinh(\eta)\cosh\left(\dfrac{\eta}{n}\right) \end{bmatrix} = 0, \tag{77}$$

with ${l_c}^2 = \dfrac{a^2}{12}$, by solving Eq. (77), one obtains

$$4\sin(\beta)\sinh(\eta)\left[\cosh\left(\frac{\eta}{n}\right) - \cos\left(\frac{\beta}{n}\right)\right]^2 = 0, \tag{78a}$$

$$\sin(\beta) = 0 \quad \text{or} \quad \sinh(\eta) = 0 \quad \text{or} \quad \cosh\left(\frac{\eta}{n}\right) - \cos\left(\frac{\beta}{n}\right) = 0. \tag{78b}$$

Therefore

$$\beta = k\pi \quad \text{or} \quad \eta = 0 \quad \text{or} \quad \cosh\left(\frac{\eta}{n}\right) = \cos\left(\frac{\beta}{n}\right). \tag{79}$$

With Eqs. (71) above, only $\beta = k\pi$ leads to a non-trivial solution. ω can be expressed as

$$\omega^2 = \frac{EI\left(\frac{k\pi}{L}\right)^4}{\rho A\left[\frac{a^2}{6}\left(\frac{k\pi}{L}\right)^2+1\right]} = \frac{EI\left(\frac{k\pi}{L}\right)^4}{\rho A\left[\frac{1}{6}\left(\frac{k\pi}{n}\right)^2+1\right]}, \tag{80}$$

which is identical to Eq. (75). k is set to 1 which corresponds to the first mode. With the increase of n, the values of Ω_1 of the first mode of lattice beam and the nonlocal approximation when $k = 1$ can be seen in Fig. 12. When n equals to 20, $\Omega_1 = 9.8512$ for the nonlocal approximation which is close to that of a continuous Euler–Bernoulli beam whose $\Omega_{1,\infty} = \pi^2 = 9.8696$ given in [32, 33].

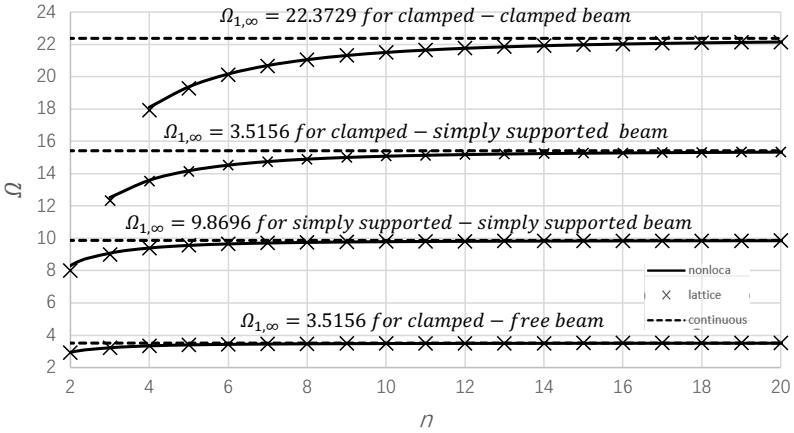

Fig. 12. Comparison of eigen value Ω_1 of the first mode with an increase of n for nonlocal/lattice/continuous beams of simply supported-simply supported/clamped-clamped/clamped-free/simply supported-clamped

4.2. For clamped-clamped beam

For a clamped-clamped nonlocal beam, the non-dimensional boundary conditions can be expressed as

$$\begin{cases} \overline{v}(0) = 0 \\ \overline{v}(1) = 0 \\ \overline{\theta}\left(\frac{1}{2n}\right) + \overline{\theta}\left(-\frac{1}{2n}\right) = 0 \Rightarrow \overline{v}\left(\frac{1}{n}\right) = \overline{v}\left(-\frac{1}{n}\right) \\ \overline{\theta}\left(1+\frac{1}{2n}\right) + \overline{\theta}\left(1-\frac{1}{2n}\right) = 0 \Rightarrow \overline{v}\left(1+\frac{1}{n}\right) = \overline{v}\left(1-\frac{1}{n}\right) \end{cases} \tag{81}$$

Coupling Eq. (71a) with Eq. (81) and setting the determinant of homogeneous coefficient matrix to zero in order to make the expression of v_i meaningful, one gets

$$\begin{bmatrix} 1 & 0 & 1 & 0 \\ \cos(\beta) & \sin(\beta) & \cosh(\eta) & \sinh(\eta) \\ 0 & 2\sin\left(\frac{\beta}{n}\right) & 0 & 2\sinh\left(\frac{\eta}{n}\right) \\ -2\sin(\beta)\sin\left(\frac{\beta}{n}\right) & 2\cos(\beta)\sin\left(\frac{\beta}{n}\right) & 2\sinh(\eta)\sinh\left(\frac{\eta}{n}\right) & 2\cosh(\eta)\sinh\left(\frac{\eta}{n}\right) \end{bmatrix} = 0. \tag{82}$$

Eq. (82) can be simplified as

$$[2-2\cos(\beta)\cosh(\eta)]\sin\left(\frac{\beta}{n}\right)\sinh\left(\frac{\eta}{n}\right)+\left[\sinh^2\left(\frac{\eta}{n}\right)-\sin^2\left(\frac{\beta}{n}\right)\right]\sinh(\eta)\sin(\beta)=0. \tag{83}$$

By coupling Eqs. (71) with Eq. (83), one can find the Ω value by a function of k and n.

k is set to 1 which corresponds to the first mode. With the increase of n, the values of Ω_1 of the first mode of lattice beam and the nonlocal approximation when $k=1$ can be seen in Fig. 12. When n equals to 20, $\Omega_1 = 22.1669$ for the nonlocal approximation is close to that of a continuous Euler–Bernoulli beam whose $\Omega_{1,\infty} = 22.3729$ given in [32,33].

4.3. For clamped-free beam

For a clamped-free nonlocal beam, the non-dimensional boundary conditions can be expressed as

$$\begin{cases} \overline{v}(0)=0 \\ \overline{\theta}\left(\frac{1}{2n}\right)+\overline{\theta}\left(-\frac{1}{2n}\right)=0 \Rightarrow \overline{v}\left(\frac{1}{n}\right)=\overline{v}\left(-\frac{1}{n}\right) \\ \overline{M}(1)=0 \Rightarrow \overline{v}\left(1+\frac{1}{n}\right)-2\overline{v}(1)+\overline{v}\left(1-\frac{1}{n}\right)=0 \\ \overline{M}\left(1+\frac{1}{n}\right)-\overline{M}\left(1-\frac{1}{n}\right)=0 \Rightarrow \overline{v}\left(1+\frac{2}{n}\right)-2\overline{v}\left(1+\frac{1}{n}\right)+2\overline{v}\left(1-\frac{1}{n}\right)-\overline{v}\left(1-\frac{2}{n}\right)=0 \end{cases} \tag{84}$$

Coupling Eq. (71a) with Eq. (84) and setting the determinant of homogeneous coefficient matrix to zero in order to make the expression of v_i meaningful, one gets

$$\begin{bmatrix} 1 & 0 & 1 & 0 \\ 0 & 2\sin\left(\frac{\beta}{n}\right) & 0 & 2\sinh\left(\frac{\eta}{n}\right) \\ 2\cos(\beta)\left(\cos\left(\frac{\beta}{n}\right)-1\right) & 2\sin(\beta)\left(\cos\left(\frac{\beta}{n}\right)-1\right) & 2\cosh(\eta)\left(\cosh\left(\frac{\eta}{n}\right)-1\right) & 2\sinh(\eta)\left(\cosh\left(\frac{\eta}{n}\right)-1\right) \\ G_1 & G_2 & G_3 & G_4 \end{bmatrix} = 0,$$

$$
\begin{aligned}
G_1 &= 4\sin\beta\sin\left(\frac{\beta}{n}\right)\left(1-\cos\left(\frac{\beta}{n}\right)\right),\\
G_2 &= 4\cos\beta\sin\left(\frac{\beta}{n}\right)\left(\cos\left(\frac{\beta}{n}\right)-1\right),\\
G_3 &= 4\sinh\eta\sinh\left(\frac{\eta}{n}\right)\left(\cosh\left(\frac{\eta}{n}\right)-1\right),\\
G_4 &= 4\cosh\eta\sinh\left(\frac{\eta}{n}\right)\left(\cosh\left(\frac{\eta}{n}\right)-1\right).
\end{aligned}
\tag{85}
$$

By coupling Eqs. (71) with Eq. (85), one can find the Ω value by a function of k and n.

k is set to 1 which corresponds to the first mode. With the increase of n, the values of Ω_1 of the first mode of lattice beam and the nonlocal approximation when $k=1$ can be seen in Fig. 12. When n equals to 20, $\Omega_1 = 3.5093$ for the nonlocal approximation is close to that of a continuous Euler–Bernoulli beam whose $\Omega_{1,\infty} = 3.5156$ given in [32,33]. Challamel et al. [14] also found the values of Ω_1 between 3.50 and 3.52.

4.4. For clamped-simply supported beam

For a clamped-simply supported nonlocal beam, the non-dimensional boundary conditions can be expressed as

$$
\begin{cases}
\overline{v}(0) = 0\\
\overline{v}(1) = 0\\
\overline{\theta}\left(\dfrac{1}{2n}\right)+\overline{\theta}\left(-\dfrac{1}{2n}\right)=0\Rightarrow\overline{v}\left(\dfrac{1}{n}\right)=\overline{v}\left(-\dfrac{1}{n}\right)\\
\overline{M}(1)=0\Rightarrow\overline{v}\left(1+\dfrac{1}{n}\right)+\overline{v}\left(1-\dfrac{1}{n}\right)=0
\end{cases}
\tag{86}
$$

Coupling Eq. (71a) with Eq. (86) and setting the determinant of homogeneous coefficient matrix to zero in order to make the expression of v_i meaningful, one gets

$$
\begin{bmatrix}
1 & 0 & 1 & 0\\
\cos(\beta) & \sin(\beta) & \cosh(\eta) & \sinh(\eta)\\
0 & 2\sin\left(\dfrac{\beta}{n}\right) & 0 & 2\sinh\left(\dfrac{\eta}{n}\right)\\
2\cos(\beta)\cos\left(\dfrac{\beta}{n}\right) & 2\sin(\beta)\cos\left(\dfrac{\beta}{n}\right) & 2\cosh(\eta)\cosh\left(\dfrac{\eta}{n}\right) & 2\sinh(\eta)\cosh\left(\dfrac{\eta}{n}\right)
\end{bmatrix}=0.
\tag{87}
$$

Eq. (87) can be simplified as

$$
4\left[\sin\left(\frac{\beta}{n}\right)\cos(\beta)\sinh(\eta)-4\sinh\left(\frac{\eta}{n}\right)\cosh(\eta)\sin(\beta)\right]\left[\cosh\left(\frac{\eta}{n}\right)-\cos\left(\frac{\beta}{n}\right)\right]=0.
\tag{88}
$$

By coupling Eqs. (71) with Eq. (88), one can find the Ω value by a function of k and n.

k is set to 1 which corresponds to the first mode. With the increase of n, the values of Ω_1 of the first mode of lattice beam and the nonlocal approximation when $k=1$ can be seen in Fig. 12. When n equals to 20, $\Omega_1 = 15.3395$ for the nonlocal approximation is close to that of a continuous Euler–Bernoulli beam whose $\Omega_{1,\infty} = 15.4182$ given in [32,

33]. Exact formula of eigenfrequencies of continualized nonlocal Euler-Bernoulli beams under various nonlocal boundary conditions (including the hinge-hinge, clamped-free, clamped-clamped and clamped-hinge boundary conditions) are available in Wang et al (2017). [34].

5. STOCHASTICS ANALYSIS OF NONLOCAL BEAMS

The idea of the stochastics analysis for nonlocal beam are similar to those of the stochastics analysis of lattice beams.

5.1. For simply supported-simply supported beam

Based on Eq. (79), the circular eigenfrequency of the first mode is

$$\omega_1{}^2 = \frac{EI\left(\frac{\pi}{n}\right)^4}{\rho A\left[\frac{1}{6}\left(\frac{\pi}{n}\right)^2+1\right]}. \tag{89}$$

The reliability R of the beam can be defined as the probability that the square of this fundamental frequency is less than the square of an excitation frequency

$$R = Prob\left\{\frac{EI\left(\frac{\pi}{n}\right)^4}{\rho A\left[\frac{1}{6}\left(\frac{\pi}{n}\right)^2+1\right]} < \omega_0{}^2\right\} = Prob\left\{EI < \frac{\omega_0{}^2 L^4 \rho A\left[\frac{1}{6}\left(\frac{\pi}{n}\right)^2+1\right]}{\pi^4}\right\}, \tag{90a}$$

$$R = F_{EI}\left\{\frac{\omega_0{}^2 L^4 \rho A\left[\frac{1}{6}\left(\frac{\pi}{n}\right)^2+1\right]}{\pi^4}\right\}, \tag{90b}$$

where F_{EI} is the probability distribution function of EI.

Coupling Eq. (46) with Eq. (90a) and Eq. (90b), the expression of the reliability for a nonlocal beam is

$$R_{nonlocal} = 1 - \exp\left[-\frac{1}{M[EI]}\frac{\omega_0{}^2 L^4 \rho A\left[\frac{1}{6}\left(\frac{\pi}{n}\right)^2+1\right]}{\pi^4}\right]. \tag{91}$$

Coupling Eq. (43) and Eq. (91), we find that the only difference between $R_{nonlocal}$ and R_{local} is the factor $\frac{1}{6}\left(\frac{\pi}{n}\right)^2+1$. By setting $R_{local} = r_0$ where r_0 is the codified reliability value, the relationship between $R_{nonlocal}$ and r_0 is

$$R_{nonlocal} = 1 - (1-r_0)^{\left[\frac{1}{6}\left(\frac{\pi}{n}\right)^2+1\right]}. \tag{92}$$

The probability of failure is conceptually opposite to the reliability

$$P_{nonlocal} = 1 - R_{nonlocal}. \tag{93}$$

By coupling Eq. (92) along with Eq. (93), the relationship between $P_{nonlocal}$ and p_0 is

$$P_{nonlocal} = 1 - R_{nonlocal} = p_0{}^{\left[\frac{1}{6}\left(\frac{\pi}{n}\right)^2+1\right]}. \tag{94}$$

The ratio of $P_{nonlocal}$ to p_0 can be expressed as a function of n

$$\frac{P_{nonlocal}}{p_0} = \frac{p_0^{\left[\frac{1}{6}\left(\frac{\pi}{n}\right)^2+1\right]}}{p_0} = p_0^{\frac{1}{6}\left(\frac{\pi}{n}\right)^2}. \tag{95}$$

With the increase of n, when p_0 equals to 0.1, 0.01 and 0.001, the values of $P_{nonlocal}$ can be seen in Fig. 13. And the values of $P_{nonlocal}/p_0$ could be seen in Fig. 14.

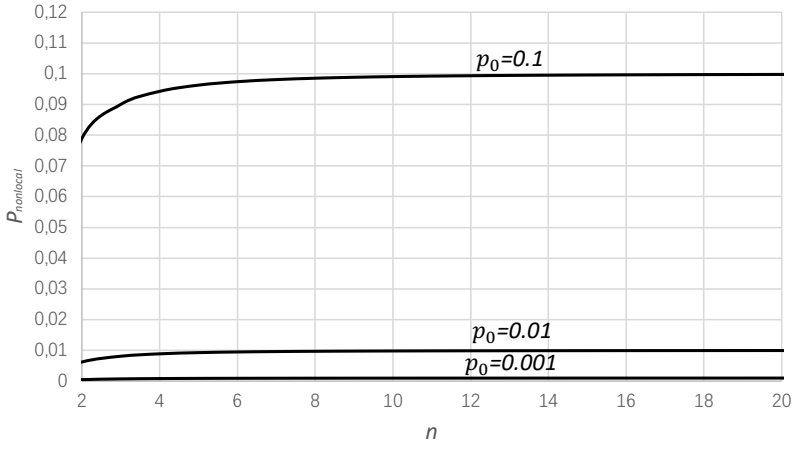

Fig. 13. Ratio of probability of failure of simply supported-simply supported nonlocal beam to probability of failure of a corresponding simply supported-simply supported Euler–Bernoulli beam $p_0 \in \{0.1,\ 0.01,\ 0.001\}$

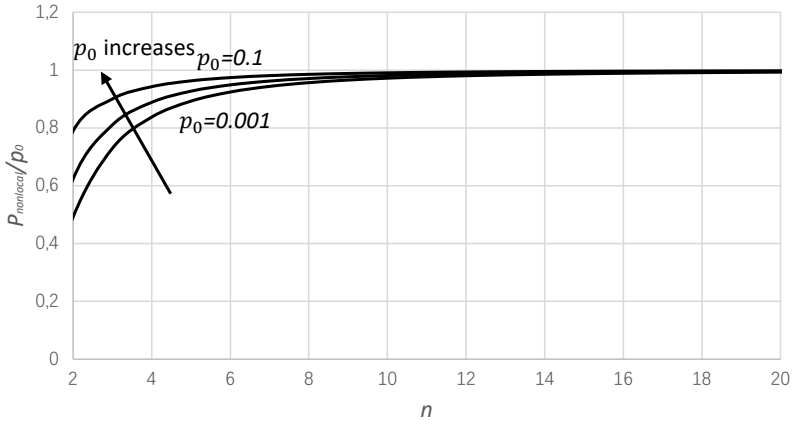

Fig. 14. Ratio of probability of failure of simply supported-simply supported nonlocal beam to probability of failure of a corresponding simply supported-simply supported Euler–Bernoulli beam $p_0 \in \{0.1,\ 0.01,\ 0.001\}$

When $p_0 = 0.01$, we compare the probabilities of failure of lattice beam and nonlocal beam with an increasing number of segments n shown in Fig. 15.

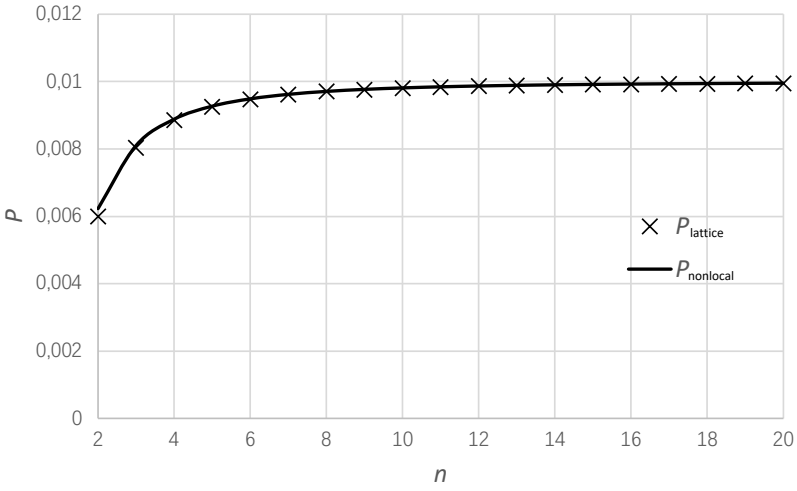

Fig. 15. Comparison between probability of failure for simply supported-simply supported nonlocal/lattice beams with an increasing n when the probability of failure of a corresponding simply supported-simply supported Euler–Bernoulli beam $p_0 = 0.01$

5.2. For clamped-clamped beam

The expression of the reliability for a nonlocal beam is

$$R_{nonlocal} = 1 - \exp\left[-\frac{1}{M\,[EI]}\frac{{\omega_0}^2 L^4 \rho A}{\Omega_1^2\,(n)}\right]. \tag{96}$$

By setting $R_{local} = r_0$ where r_0 is the codified reliability value and by coupling Eq. (96) with Eq. (53a) and Eq. (53b), the relationship between $R_{nonlocal}$ and r_0 is

$$1 - R_{nonlocal} = \exp\left[-\frac{1}{M[EI]}\frac{{\omega_0}^2 L^4 \rho A}{\Omega_1^2(n)}\right] = (1 - R_{local})^{\frac{\Omega_{1,\infty}^2}{\Omega_1^2(n)}}, \tag{97a}$$

$$R_{nonlocal} = 1 - (1 - r_0)^{\frac{\Omega_{1,\infty}^2}{\Omega_1^2(n)}}. \tag{97b}$$

By coupling Eq. (97b) along with Eq. (54), the relationship between $P_{nonlocal}$ and p_0 is

$$P_{nonlocal} = 1 - R_{nonlocal} = {p_0}^{\frac{\Omega_{1,\infty}^2}{\Omega_1^2(n)}}. \tag{98}$$

The ratio of $P_{nonlocal}$ to p_0 can be expressed as a function of n

$$\frac{P_{nonlocal}}{p_0} = \frac{{p_0}^{\frac{\Omega_{1,\infty}^2}{\Omega_1^2(n)}}}{p_0} = {p_0}^{\frac{\Omega_{1,\infty}^2}{\Omega_1^2(n)}-1}. \tag{99}$$

With the increase of n, when p_0 equals to 0.1, 0.01 and 0.001, the values of $P_{nonlocal}$ can be seen in Fig. 16. The values of $P_{nonlocal}/p_0$ can be seen in Fig. 17.

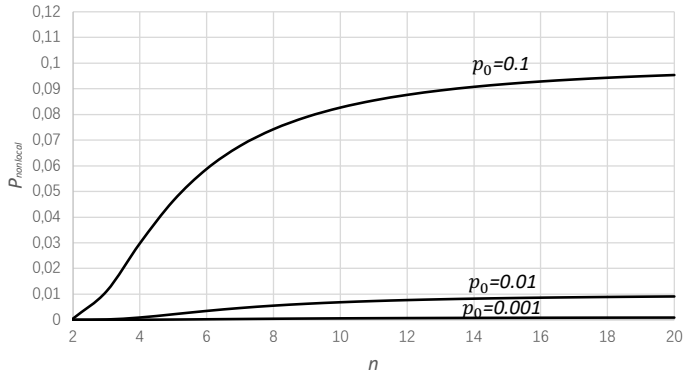

Fig. 16. Ratio of probability of failure of clamped-clamped nonlocal beam to probability of failure of a corresponding clamped-clamped Euler–Bernoulli beam $p_0 \in \{0.1,\ 0.01,\ 0.001\}$

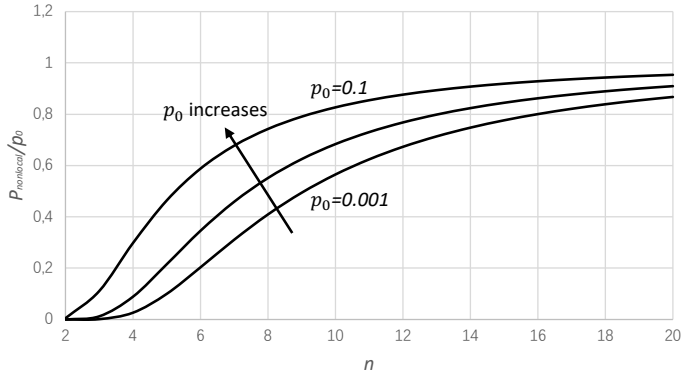

Fig. 17. Ratio of probability of failure of clamped-clamped nonlocal beam to probability of failure of a corresponding clamped-clamped Euler–Bernoulli beam $p_0 \in \{0.1,\ 0.01,\ 0.001\}$

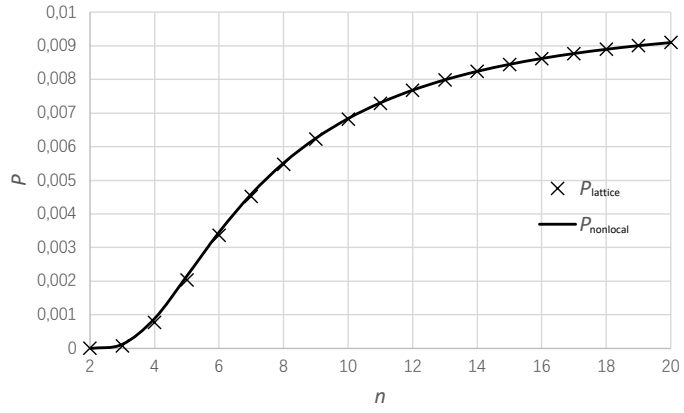

Fig. 18. Comparison between probability of failure for clamped-clamped nonlocal/lattice beams with an increasing n when the probability of failure of a corresponding clamped-clamped Euler–Bernoulli beam $p_0 = 0.01$

When $p_0 = 0.01$, we compare the probabilities of failure of lattice beam and nonlocal beam with an increasing the number of segments n in Fig. 18.

5.3. For clamped-free beam

For a clamped-free beam, the relationship between $P_{nonlocal}$ and p_0 is also given by Eq. (99), with the equations of $\Omega_{1,\infty}$ given by Eq. (56a) and Eq. (56b). With the increase of n, when p_0 equals to 0.1, 0.01 and 0.001, the values of $P_{nonlocal}$ can be seen in Fig. 19. The values of $P_{nonlocal}/p_0$ can be seen in Fig. 20.

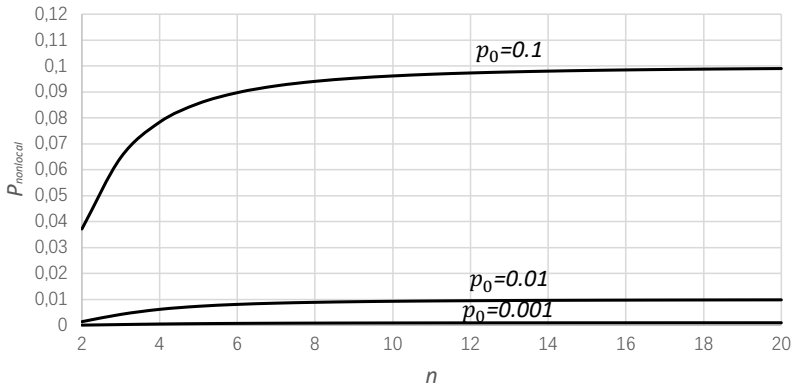

Fig. 19. Ratio of probability of failure of clamped-free nonlocal beam to probability of failure of a corresponding clamped-free Euler–Bernoulli beam $p_0 \in \{0.1,\ 0.01,\ 0.001\}$

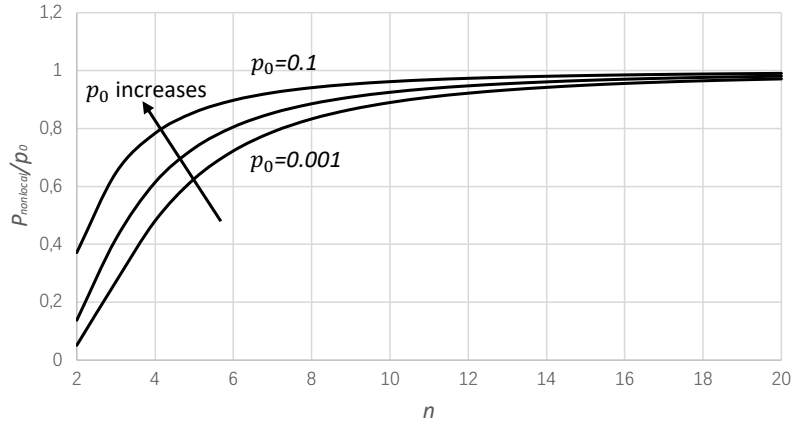

Fig. 20. Ratio of probability of failure of clamped-free nonlocal beam to probability of failure of a corresponding clamped-free Euler–Bernoulli beam $p_0 \in \{0.1,\ 0.01,\ 0.001\}$

When $p_0 = 0.01$, we compare the probabilities of failure of lattice beam and nonlocal beam with an increasing number of segments n in Fig. 21.

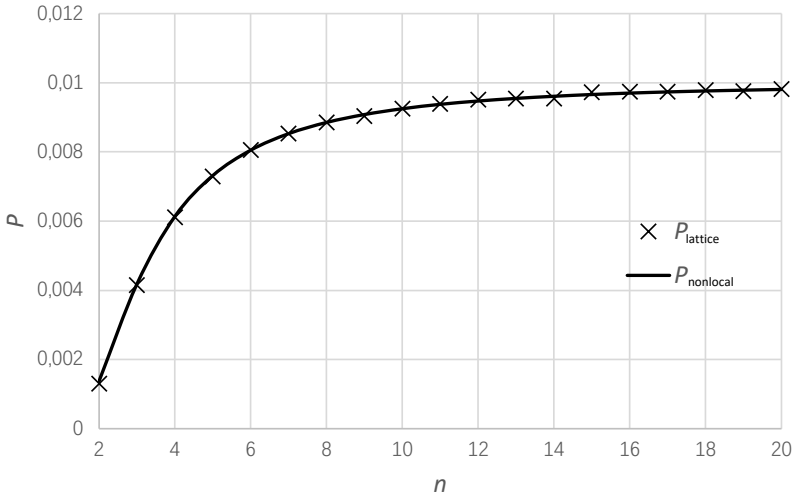

Fig. 21. Comparison between probability of failure for clamped-free nonlocal/lattice beams with an increasing n when the probability of failure of a corresponding clamped-free Euler–Bernoulli beam $p_0 = 0.01$

5.4. For clamped-simply supported beam

For a clamped-simply supported beam, the relationship between $P_{nonlocal}$ and p_0 is also given by Eq. (99), with the equations of $\Omega_{1,\infty}$ given by Eq. (57a) and Eq. (57b). With the increase of n, when p_0 equals to 0.1, 0.01 and 0.001, the values of $P_{nonlocal}$ can be seen in Fig. 22. And the values of $P_{nonlocal}/p_0$ can be seen in Fig. 23.

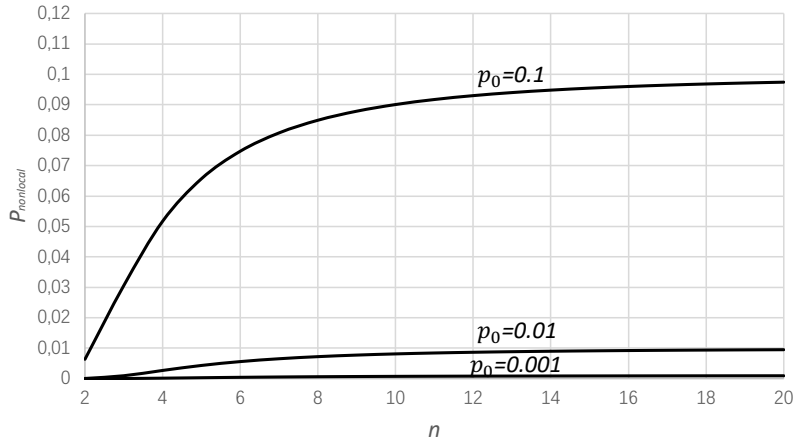

Fig. 22. Ratio of probability of failure of clamped-simply supported nonlocal beam to probability of failure of a corresponding clamped-simply supported Euler–Bernoulli beam $p_0 \in \{0.1,\ 0.01,\ 0.001\}$

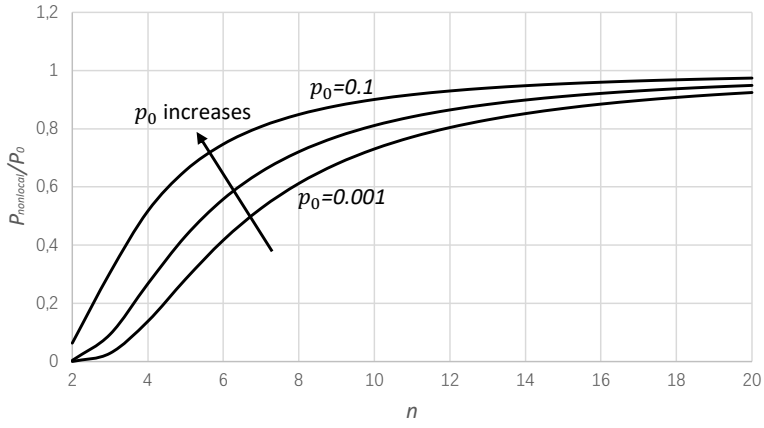

Fig. 23. Ratio of probability of failure of clamped-simply supported nonlocal beam to probability of failure of a corresponding clamped-simply supported Euler–Bernoulli beam $p_0 \in \{0.1,\ 0.01,\ 0.001\}$

When $p_0 = 0.01$, we compare the probabilities of failure of lattice beam and nonlocal beam with an increasing number of segments n in Fig. 24.

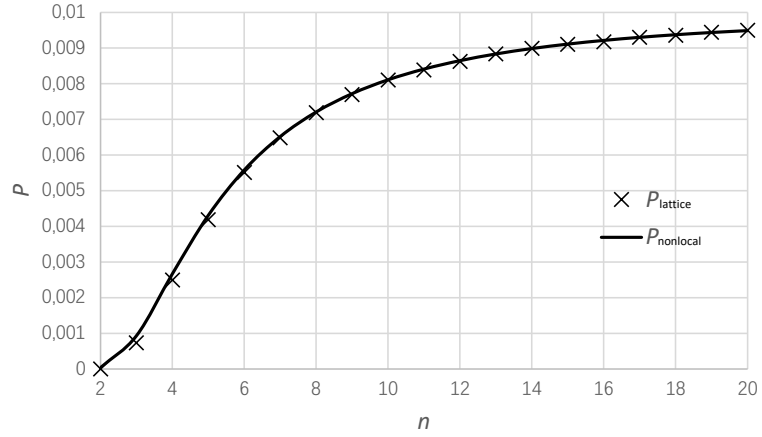

Fig. 24. Comparison between probability of failure for clamped-simply supported nonlocal/lattice beams with an increasing n when the probability of failure of a corresponding clamped-simply supported Euler–Bernoulli beam $p_0 = 0.01$

6. CONCLUSION

This paper studies the structural reliability for Hencky bar-chain model under free vibration with its nonlocal approximations. It is shown that the accuracy strongly depends on the number of segments. With an increasing number of segments, the eigenvalues and the probabilities of failure of elastic Hencky bar-chain models and elastic

Eringen's nonlocal approximation models both approach to those of continuous Euler–Bernoulli beams at the same rate. The nonlocal Euler–Bernoulli beam model is an efficient continuous model for investigating lattice beam problems in both deterministic and non-deterministic frame work.

REFERENCES

[1] A. K. Noor. Continuum modeling for repetitive lattice structures. *Applied Mechanics Reviews*, **41**, (1988), pp. 285–296. https://doi.org/10.1115/1.3151907.

[2] M. Ostoja-Starzewski. Lattice models in micromechanics. *Applied Mechanics Reviews*, **55**, (2002), pp. 35–60. https://doi.org/10.1115/1.1432990.

[3] H. Hencky. Über die angenäherte Lösung von Stabilitätsproblemen im Raum mittels der elastischen Gelenkkette. *Der Eisenbau*, **11**, (1920), pp. 437–452.

[4] M. G. Salvadori. Numerical computation of buckling loads by finite differences. *Transactions of the American Society of Civil Engineers*, **116**, (1951), pp. 590–624. https://doi.org/10.1061/taceat.0006570.

[5] F. A. Leckie and G. M. Lindberg. The effect of lumped parameters on beam frequencies. *Aeronautical Quarterly*, **14**, (1963), pp. 224–240. https://doi.org/10.1017/s0001925900002791.

[6] M. S. El Naschie and S. Stress. *Chaos in structural engineering: An energy approach*. McGraw Hil, New York, (1990).

[7] H. Zhang, C. M. Wang, E. Ruocco, and N. Challamel. Hencky bar-chain model for buckling and vibration analyses of non-uniform beams on variable elastic foundation. *Engineering Structures*, **126**, (2016), pp. 252–263. https://doi.org/10.1016/j.engstruct.2016.07.062.

[8] R. K. Livesley. The equivalence of continuous and discrete mass distributions in certain vibration problems. *The Quarterly Journal of Mechanics and Applied Mathematics*, **8**, (3), (1955), pp. 353–360. https://doi.org/10.1093/qjmam/8.3.353.

[9] M. G. Salvadori. Numerical computation of buckling loads by finite differences. *Transactions of the American Society of Civil Engineers*, **116**, (1951), pp. 590–624. https://doi.org/10.1061/taceat.0006570.

[10] T. Wah and L. R. Calcote. *Structural analysis by finite difference calculus*. Van Nostrand Reinhold Company, (1970).

[11] C. M. Wang, H. Zhang, R. P. Gao, W. H. Duan, and N. Challamel. Hencky bar-chain model for buckling and vibration of beams with elastic end restraints. *International Journal of Structural Stability and Dynamics*, **15**, (2015), p. 1540007. https://doi.org/10.1142/s0219455415400076.

[12] I. Elishakoff and R. Santoro. Error in the finite difference based probabilistic dynamic analysis: analytical evaluation. *Journal of Sound and Vibration*, **281**, (2005), pp. 1195–1206. https://doi.org/10.1016/j.jsv.2004.03.066.

[13] R. Santoro and I. Elishakoff. Accuracy of the finite difference method in stochastic setting. *Journal of Sound and Vibration*, **291**, (2006), pp. 275–284. https://doi.org/10.1016/j.jsv.2005.06.038.

[14] N. Challamel, Z. Zhang, C. M. Wang, J. N. Reddy, Q. Wang, T. Michelitsch, and B. Collet. On nonconservativeness of Eringen's nonlocal elasticity in beam mechanics: correction from a discrete-based approach. *Archive of Applied Mechanics*, **84**, (2014), pp. 1275–1292. https://doi.org/10.1007/s00419-014-0862-x.

[15] Z. Zhang, C. M. Wang, N. Challamel, and I. Elishakoff. Obtaining Eringen's length scale coefficient for vibrating nonlocal beams via continualization method. *Journal of Sound and Vibration*, **333**, (2014), pp. 4977–4990. https://doi.org/10.1016/j.jsv.2014.05.002.

[16] I. Elishakoff and C. Soize. *Nondeterministic mechanics*. International Centre for Mechanical Sciences, Courses and Lectures - No. 539, SpringerWienNewYork, (2012).
[17] E. Vanmarcke and M. Grigoriu. Stochastic finite element analysis of simple beams. *Journal of Engineering Mechanics*, **109**, (1983), pp. 1203–1214. https://doi.org/10.1061/(asce)0733-9399(1983)109:5(1203).
[18] K. Gao, W. Gao, D. Wu, and C. Song. Nonlinear dynamic stability analysis of Euler–Bernoulli beam–columns with damping effects under thermal environment. *Nonlinear Dynamics*, **90**, (2017), pp. 2423–2444. https://doi.org/10.1007/s11071-017-3811-8.
[19] K. Gao, W. Gao, B. Wu, and C. Song. Nondeterministic dynamic stability assessment of Euler–Bernoulli beams using Chebyshev surrogate model. *Applied Mathematical Modelling*, **66**, (2019), pp. 1–25. https://doi.org/10.1016/j.apm.2018.09.007.
[20] K. Gao, R. Li, and J. Yang. Dynamic characteristics of functionally graded porous beams with interval material properties. *Engineering Structures*, **197**, (2019), p. 109441. https://doi.org/10.1016/j.engstruct.2019.109441.
[21] S. Kukla and A. Owczarek. Stochastic vibration of a Bernoulli–Euler beam under random excitation. *Scientific Research of the Institute of Mathematics and Computer Science*, **4**, (1), (2005), pp. 71–78.
[22] C. R. A. Silva Junior, A. T. Beck, and E. Rosa. Solution of the stochastic beam bending problem by Galerkin method and the Askey-Wiener scheme. *Latin American Journal of Solids and Structures*, **6**, (2009), pp. 51–72.
[23] A. C. Eringen. On differential equations of nonlocal elasticity and solutions of screw dislocation and surface waves. *Journal of Applied Physics*, **54**, (1983), pp. 4703–4710. https://doi.org/10.1063/1.332803.
[24] J. A. D. Wattis. Quasi-continuum approximations to lattice equations arising from the discrete nonlinear telegraph equation. *Journal of Physics A: Mathematical and General*, **33**, (2000), pp. 5925–5944. https://doi.org/10.1088/0305-4470/33/33/311.
[25] I. V. Andrianov, J. Awrejcewicz, and D. Weichert. Improved continuous models for discrete media. *Mathematical Problems in Engineering*, **2010**, (2010), pp. 1–35. https://doi.org/10.1155/2010/986242.
[26] W. H. Duan, N. Challamel, C. M. Wang, and Z. Ding. Development of analytical vibration solutions for microstructured beam model to calibrate length scale coefficient in nonlocal Timoshenko beams. *Journal of Applied Physics*, **114**, (2013), p. 104312. https://doi.org/10.1063/1.4820565.
[27] N. Challamel, Z. Zhang, and C. M. Wang. Nonlocal equivalent continua for buckling and vibration analyses of microstructured beams. *Journal of Nanomechanics and Micromechanics*, **5**, (2015). https://doi.org/10.1061/(asce)nm.2153-5477.0000062.
[28] J. N. Reddy. Nonlocal theories for bending, buckling and vibration of beams. *International Journal of Engineering Science*, **45**, (2007), pp. 288–307. https://doi.org/10.1016/j.ijengsci.2007.04.004.
[29] N. Challamel, C. M. Wang, and I. Elishakoff. Discrete systems behave as nonlocal structural elements: Bending, buckling and vibration analysis. *European Journal of Mechanics - A/Solids*, **44**, (2014), pp. 125–135. https://doi.org/10.1016/j.euromechsol.2013.10.007.
[30] V. D. Potapov. Stability via nonlocal continuum mechanics. *International Journal of Solids and Structures*, **50**, (2013), pp. 637–641. https://doi.org/10.1016/j.ijsolstr.2012.10.019.
[31] G. Alotta, M. D. Paola, G. Failla, and F. P. Pinnola. On the dynamics of non-local fractional viscoelastic beams under stochastic agencies. *Composites Part B: Engineering*, **137**, (2018), pp. 102–110. https://doi.org/10.1016/j.compositesb.2017.10.014.

[32] C. Y. Wang and C. M. Wang. *Structural vibration: exact solutions for strings, membranes, beams, and plates*. CRC Press, (2019).

[33] R. D. Blevins. *Formulas for dynamics, acoustics and vibration*, chapter 4, pp. P139–P140. John Wiley & Sons, Ltd, (2015). https://doi.org/10.1002/9781119038122.

[34] C. M. Wang, H. Zhang, N. Challamel, and W. H. Duan. On boundary conditions for buckling and vibration of nonlocal beams. *European Journal of Mechanics-A/Solids*, **61**, (2017), pp. 73–81. https://doi.org/10.1016/j.euromechsol.2016.08.014.

[35] C. M. Wang, H. Zhang, N. Challamel, and W. Pan. *Hencky Bar-chain/net for Structural Analysis*. World Scientific, (2020).

[36] I. Elishakoff. Prologue. In *Safety factors and reliability: Friends or foes?*, pp. 1–11. Springer Netherlands, (2004). https://doi.org/10.1007/978-1-4020-2131-2_1.

[37] N. Challamel, V. Picandet, B. Collet, T. Michelitsch, I. Elishakoff, and C. M. Wang. Revisiting finite difference and finite element methods applied to structural mechanics within enriched continua. *European Journal of Mechanics - A/Solids*, **53**, (2015), pp. 107–120. https://doi.org/10.1016/j.euromechsol.2015.03.003.